Magnetic and compositional order in nickel-rich Ni_cFe_{1-c} alloys

1991 J. Phys.: Condens. Matter 3 1575

(http://iopscience.iop.org/0953-8984/3/11/016)

J. Phys.: Condens. Matter 3 (1991) 1575–1587. Printed in the UK

Magnetic and compositional order in nickel-rich Ni_cFe_{1-c} alloys

M B Taylor, B L Gyorffy and C J Walden
H H Wills Physics Laboratory, Royal Fort, Tyndall Avenue, Bristol, UK

Received 25 October 1990

Abstract. The nickel-rich FCC Ni_cFe_{1-c} alloy system is modelled using a lattice with two Ising-like degrees of freedom at each site, one compositional and one magnetic. This system is investigated with both a mean field theory and computer simulation. Parameters of the model are obtained by fitting to the concentration dependence of Curie temperature observed. The simulations reproduce the observed compositional ($L1_2$) ordering in the region of interest and an associated magnetic anomaly. We confirm the conjecture that the Fe–Fe exchange coupling in this alloy is antiferromagnetic and provide an estimate of its strength.

1. Introduction

The Ni_cFe_{1-c} alloy system is of general scientific and technological interest. One of the many issues which continues to attract attention is the nature of the magnetic coupling between the Fe atoms in the Ni-rich alloys. Although there is mounting evidence [1–6] that this coupling is antiferromagnetic there is no reliable estimate of its strength. The aim of this work is to provide such an estimate.

We model the system in the nickel-rich region near $c = 0.75$ where the system is face centred cubic (FCC). Our model is not applicable below $c \approx 0.5$ where the moment collapses [7] indicating complex physical processes which are not described by our simple spin-only Hamiltonian. The main features of the experimental phase diagram (figure 1) in which we are interested are the first-order compositional transition from the $L1_2$ (Cu_3Au) structure to a chemically disordered state at the ordering temperature T_O, and the second-order ferromagnetic/paramagnetic transition at a higher Curie temperature T_C.

The simplest possible model which incorporates both magnetic and compositional degrees of freedom is given by the following effective Hamiltonian:

$$\mathcal{H} = -\sum_{i>j}\left[\xi_i\xi_j J_{ij}^{\mathrm{NiNi}} + \xi_i(1-\xi_j)J_{ij}^{\mathrm{NiFe}} + (1-\xi_i)\xi_j J_{ij}^{\mathrm{NiFe}} + (1-\xi_i)(1-\xi_j)J_{ij}^{\mathrm{FeFe}}\right]\sigma_i\sigma_j - \sum_i \nu_i\xi_i - \sum_{i>j} V_{ij}\xi_i\xi_j \qquad (1)$$

where the occupation variable $\xi_i = 1$ if there is a Ni atom at the site i and $\xi_i = 0$ if the site is occupied by an Fe atom, and σ_i is an Ising spin variable $\sigma_i = \pm 1$. Moreover, in an obvious notation J_{ij}^{NiNi}, J_{ij}^{NiFe} and J_{ij}^{FeFe} are exchange integrals, V_{ij} is a chemical

0953-8984/91/111575+13$03.50

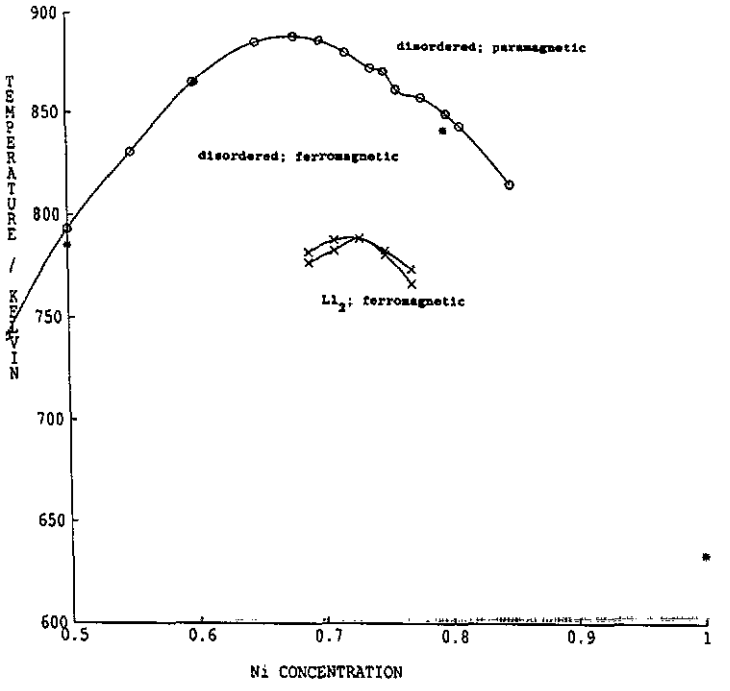

Figure 1. Experimental phase diagram of the Ni_cFe_{1-c} system. *, T_C data of Crangle and Hallam [10]; O, T_C data of Wakelin and Yates [13]; ×, T_O data of Van Deen and Van der Woude [14].

interchange energy ($\sim V_{ij}^{\mathrm{NiNi}} + V_{ij}^{\mathrm{FeFe}} - 2V_{ij}^{\mathrm{NiFe}}$) and ν_i is a local chemical potential difference between the two species.

The nearest neighbour Ni–Ni and Ni–Fe interactions are thought to be ferromagnetic, and the nearest neighbour Fe–Fe interaction to be antiferromagnetic. This circumstance leads to an interesting interaction between the ferromagnetic and compositional orders: the overall ferromagnetism of the system tends to force the antiferromagnetic minority iron atoms on to non-adjacent sites, leading to $L1_2$ ordering near 75% nickel on a FCC lattice.

As mentioned above our main aim is to find a set of parameters $\{J_{ij}^{\mathrm{NiNi}}, J_{ij}^{\mathrm{NiFe}}, J_{ij}^{\mathrm{FeFe}}, V_{ij}\}$ which reproduce the available experimental data. For the purposes of this paper the system was considered homogeneous and isotropic; moreover no interactions at longer range than next nearest neighbour were considered. This leaves only eight parameters of the model: $J_{\mathrm{nn}}^{\mathrm{NiNi}}$, $J_{\mathrm{nn}}^{\mathrm{NiFe}}$, $J_{\mathrm{nn}}^{\mathrm{FeFe}}$, V_{nn}, $J_{\mathrm{nnn}}^{\mathrm{NiNi}}$, $J_{\mathrm{nnn}}^{\mathrm{NiFe}}$, $J_{\mathrm{nnn}}^{\mathrm{FeFe}}$, and V_{nnn}. Although next nearest neighbour interactions are thought to be relatively unimportant (but see the discussion of short range order parameters in subsection 4.3), it proved to be necessary to introduce some in order to break the degeneracy of the ground state (see [8]). These were set to a fixed fraction of the nearest neighbour interactions, large enough to break the degeneracy but small enough to have negligible other effects on the system's behaviour. In particular the interaction ratios were set as follows:

$$\frac{J_{\mathrm{nnn}}^{\mathrm{NiFe}}}{J_{\mathrm{nn}}^{\mathrm{NiFe}}} = \frac{J_{\mathrm{nnn}}^{\mathrm{FeFe}}}{J_{\mathrm{nn}}^{\mathrm{FeFe}}} = -\frac{1}{100} \qquad J_{\mathrm{nnn}}^{\mathrm{NiNi}} = V_{\mathrm{nnn}} = 0 \tag{2}$$

This leaves four free parameters of the system to be fitted to experimental data.

We have investigated the consequences of the model Hamiltonian (1) using a mean field theory and computer simulation.

2. The basic results of the mean field theory

A usual mean field theory [9] for the Hamiltonian (1) using the definitions:

$$c_i = \langle \xi_i \rangle \qquad c_i m_i^{\mathrm{Ni}} = \langle \xi_i \sigma_i \rangle \qquad (1-c_i) m_i^{\mathrm{Fe}} = \langle (1-\xi_i)\sigma_i \rangle$$

yields the following self-consistency equations:

$$m_i^{\mathrm{Ni}} = \tanh \Gamma_i^{\mathrm{N}} \tag{3}$$

$$m_i^{\mathrm{Fe}} = \tanh \Gamma_i^{\mathrm{F}} \tag{4}$$

$$c_i = \frac{e^{\beta\left(\nu_i + \sum_j V_{ij} c_j\right)} \cosh \Gamma_i^{\mathrm{N}}}{\cosh \Gamma_i^{\mathrm{F}} + e^{\beta\left(\nu_i + \sum_j V_{ij} c_j\right)} \cosh \Gamma_i^{\mathrm{N}}} \tag{5}$$

where

$$\Gamma_i^{\mathrm{N}} = \beta \sum_j \left[c_j m_j^{\mathrm{Ni}} J_{ij}^{\mathrm{NiNi}} + (1-c_j) m_j^{\mathrm{Fe}} J_{ij}^{\mathrm{NiFe}} \right]$$

$$\Gamma_i^{\mathrm{F}} = \beta \sum_j \left[c_j m_j^{\mathrm{Ni}} J_{ij}^{\mathrm{NiFe}} + (1-c_j) m_j^{\mathrm{Fe}} J_{ij}^{\mathrm{FeFe}} \right]$$

These equations were solved numerically for a FCC lattice represented as four interpenetrating simple cubic sublattices, all sites on each sublattice being regarded as equivalent. Four was chosen because it is the minimum number which allows $L1_2$ ordering. In addition we have derived a formula for the Curie temperature T_C as a function of concentration c (i.e. percentage nickel composition). It is given by

$$k_B T_C = \tfrac{1}{2}\Big[c J_{\mathrm{tot}}^{\mathrm{NiNi}} + (1-c) J_{\mathrm{tot}}^{\mathrm{FeFe}} \pm \sqrt{\left(c J_{\mathrm{tot}}^{\mathrm{NiNi}} + (1-c) J_{\mathrm{tot}}^{\mathrm{FeFe}}\right)^2 - 4c(1-c)\left(J_{\mathrm{tot}}^{\mathrm{NiNi}} J_{\mathrm{tot}}^{\mathrm{FeFe}} - J_{\mathrm{tot}}^{\mathrm{NiFe}^2}\right)} \Big] \tag{6}$$

where:

$$J_{\mathrm{tot}}^{\mathrm{XY}} = 12 J_{\mathrm{nn}}^{\mathrm{XY}} + 6 J_{\mathrm{nnn}}^{\mathrm{XY}} \tag{7}$$

there being 12 nearest and 6 next nearest neighbours on the FCC lattice. This relation holds only on the condition that the system lacks compositional long range order at the Curie temperature, i.e. for $T_C(c) > T_O(c)$; in all regions in which we are interested this is the case. This provides a single-valued function $T_C(c)$, since the option of subtracting the square root corresponds to non-physical solutions. Note that this function is dependent only on the magnetic interaction parameters $\{J_{\mathrm{tot}}^{\mathrm{XY}}\}$ and not on the chemical interaction V. This is a consequence of the fact that near T_C there is no compositional order. The results of our calculation and the consequences of (6) will be further discussed in subsection 4.1.

3. Details of the simulation

The system was simulated using the Metropolis Monte Carlo method on an AMT Distributed Array Processor 510. Runs were primarily on a $32 \times 32 \times 32$ lattice, although for assessment of finite size effects $16 \times 16 \times 16$ and $8 \times 8 \times 8$ lattices were also used. Boundary conditions were cyclic in all three directions. Runs were of between 4000 and 15000 Monte Carlo steps per site at each temperature near T_C, and between 800 and 3000 steps far from T_C, care being taken that the system had reached equilibrium before data were accumulated. Alloy composition was controlled by specifying chemical potential ν; this was very much easier to implement, and consequently much faster, on the hardware available than mimicking the natural experimental method of holding constant the percentage of nickel. The simulation ran at about 8×10^5 Monte Carlo steps per second. Quantities observed were concentration, magnetization, internal energy, specific heat, susceptibility†, order parameters pertaining to $L1_2$ and $L1_0$ order, and the nearest and next nearest neighbour correlation functions $\langle \sigma_i \sigma_j \rangle$, $\langle \xi_i \xi_j \rangle$ and $\langle \sigma_i \xi_j \rangle$.

4. Discussion and interpretation of the results

As noted above, both simulation and mean field theory results were calculated. For each quantity of interest, where possible, the predictions of the two methods were compared. In some cases, as described below, comparison of the two revealed a discrepancy, and we have endeavoured to understand these in terms of correlations not included in the mean field theory. Where it was clear that there was no significant difference between the two, the mean field theory was in general used for more detailed investigation of the system's behaviour, since this approach made much smaller demands on computer time, rendering it practicable in particular to obtain results at constant concentration, rather than at constant chemical potential as required by the simulation.

4.1. The phase diagram for the Ni-rich alloys

As mentioned above we have an analytic formula (6) for $T_C(\{J_{tot}^{XY}\}, c)$ in the mean field approximation. We fitted this to experimental results from [10] (plotted in figure 2) of the concentration dependence of the Curie temperature to find:

$$\frac{J_{tot}^{NiFe}}{J_{tot}^{NiNi}} = +2.196 \qquad \frac{J_{tot}^{FeFe}}{J_{tot}^{NiNi}} = -0.633 \tag{8}$$

where the Ni–Ni and Ni–Fe interactions are ferromagnetic and the Fe–Fe interaction is antiferromagnetic. Using the mean field value of $k_B T_C / J_{tot} = 12$ for an Ising FCC ferromagnet (i.e. the alloy Ni_1Fe_0) and the experimental value of $T_C^{Ni} = 634$ K from [11] this gives a fairly good fit in the region of interest, but this is unsurprising considering that the fit is of three unknowns to only four data points.

The simulation Curie temperature curve $T_C^{SIM}(c)$ is of almost exactly the same shape, but lower in temperature by a factor of 9.795/12 ($= T_C^{Exact}/T_C^{MFT}$ for an Ising

† Specific heat and susceptibility were determined using two forms of the fluctuation theorem, viz. $C_H = (k_B T^2)^{-1}(\langle E^2 \rangle - \langle E \rangle^2)$ and $\chi_T = (k_B T)^{-1}(\langle M^2 \rangle - \langle M \rangle^2)$.

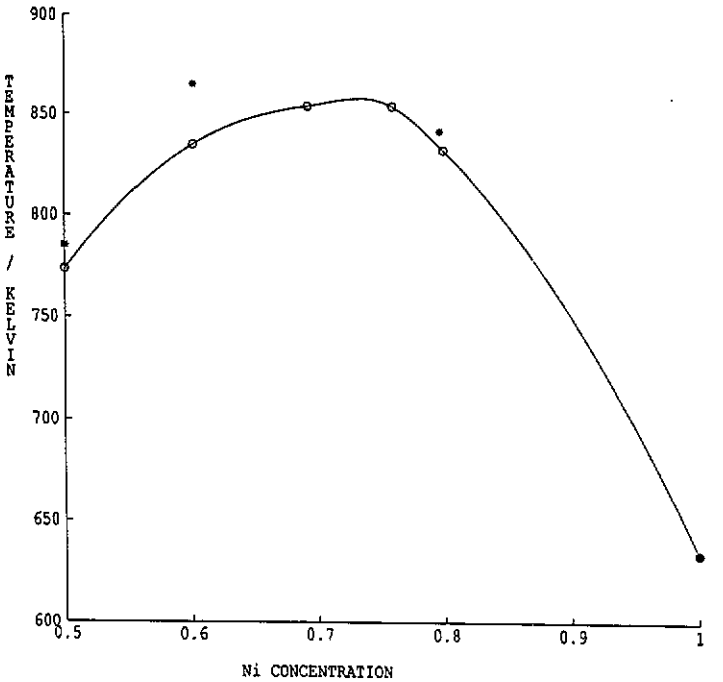

Figure 2. Curie temperature T_C of the simulation with exchange interactions determined by fitting the mean field theory to the experimental Curie temperature and with chemical interaction $V = 0$. O, simulation; *, experiment [10].

FCC ferromagnet; see [12]). So by using the value of $k_B T_C / J_{tot} = 9.795$ and the values (8) above we were able to estimate a set of exchange integrals $\{J_{tot}^{XY}\}$ for the system. A simulation using these values in conjunction with the relations given in (2) gives the $T_C(c)$ shown in figure 2.

Towards the end of the study we became aware of a more complete set of experimental values for the Curie temperature [13] (see figure 1 for a comparison of these and the data of [10]), and a fit to these is not only somewhat different to the fit to the data of [10] (a more quantitative consideration of these differences is given below), but shows that the shape of the $T_C(c)$ curve cannot be reproduced with very great accuracy by our model with any set of parameters, the experimental curve being somewhat more sharply peaked than the theoretical ones. This suggests that the model is in some ways inadequate, probably in failing to take account of the concentration dependence of one or more of the parameters of the system.

The compositional ordering temperature $T_O(c)$ was also investigated. Unlike the magnetic phase transition, the $L1_2$/disordered transition is first-order in experiment (see [14]). The transition is reproduced by the model described above, but at around $0.2T_C$ rather than at the experimental value of $0.9T_C$. As expected [15], the mean field theory and simulation differ markedly in the form of the $T_O(c)$ curve: T_O^{SIM}, like the experimental data, has a maximum close to the stoichiometric composition (75% nickel) while T_O^{MFT} increases monotonically with increasing iron concentration (figure 3), as in the well-known work of Shockley [16].

To reproduce more closely the experimental behaviour a negative chemical in-

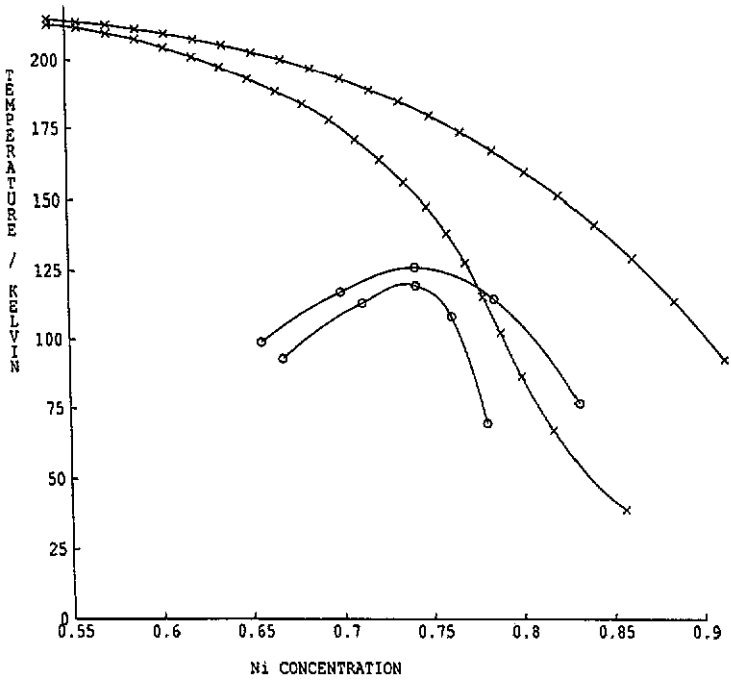

Figure 3. Ordering temperature T_O of mean field theory and simulation. Upper and lower bounds of phase stability are plotted, so that the region between the curves for each system is the region in which ordered and disordered phases may coexist. ×, Mean field approximation; ○, simulation.

teraction V was introduced. This had the effect of increasing the tendency to order compositionally, and thus of raising the ordering temperature. As long as T_O remained below T_C the general form of the $T_O(c)$ curve remained the same, monotonic in the mean field theory and peaking close to stoichiometry in the simulation. No analytic expression could be derived for $T_O(c)$, and so the fit to the experimental data was by eye and fairly rough; but in view of the Ising-like simplicity of the model it was as accurate as appropriate. A value of $V = -25J_{tot}^{NiNi}$ was chosen to fix T_O/T_C at about the right level. With this modification the simulation phase diagram in the region of interest is quite similar to the experimental one, although the shape of the region of coexistence of ordered and disordered phases differs somewhat between the two; this can be seen by comparison of figure 4 with figure 1.

Another interesting difference between the mean field theory and the simulation is that while T_C^{MFT} is independent of the chemical interaction V (see (6)), T_C^{SIM} does depend weakly on V—an increase in $-V$ from 0 to $25J_{tot}^{NiNi}$ gives an increase in T_C^{SIM} of about 10%. This is due to the persistence of some short range $L1_2$ order above T_O in the simulation, which leaves fewer antiferromagnetic iron atoms on adjacent sites than in the disordered state, thus increasing the effective exchange interaction:

$$\overline{J} = \frac{1}{N}\sum_{i>j}\left[\langle\xi_i\xi_j\rangle J_{ij}^{NiNi} + \langle\xi_i(1-\xi_j)\rangle J_{ij}^{NiFe} + \langle(1-\xi_i)\xi_j\rangle J_{ij}^{NiFe} + \langle(1-\xi_i)(1-\xi_j)\rangle J_{ij}^{FeFe}\right] \tag{9}$$

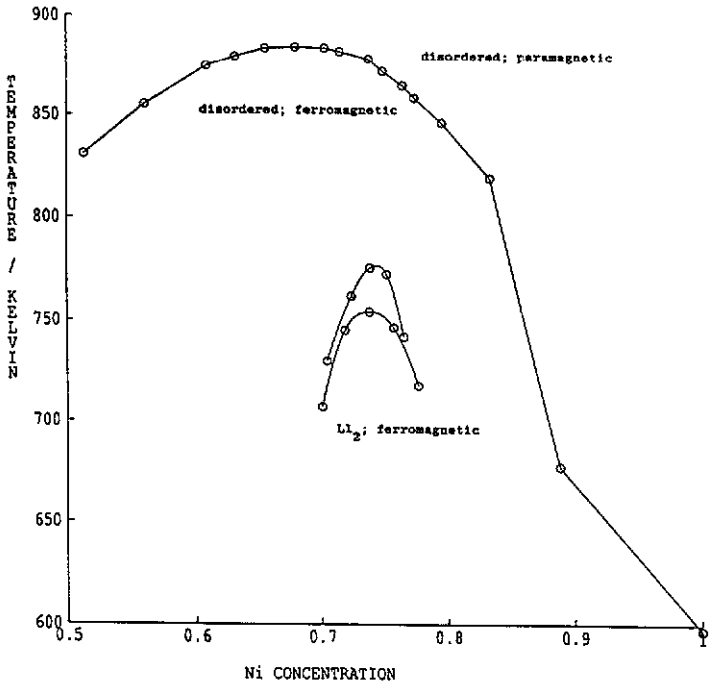

Figure 4. Phase diagram for the simulation with magnetic and chemical interactions as used for the bulk of our results.

above its disordered value:

$$\overline{J}_{\text{dis}} = \frac{1}{N}\sum_{i>j}\left[c^2 J_{ij}^{\text{NiNi}} + 2c(1-c)J_{ij}^{\text{NiFe}} + (1-c)^2 J_{ij}^{\text{FeFe}}\right]$$
$$= c^2 J_{\text{tot}}^{\text{NiNi}} + 2c(1-c)J_{\text{tot}}^{\text{NiFe}} + (1-c)^2 J_{\text{tot}}^{\text{FeFe}}. \tag{10}$$

A larger value of $\overline{J}$ increases the ferromagnetic tendency of the system and thus raises the Curie temperature. Due to the insensitivity of mean field theories to time fluctuations and the fact that a non-zero short range order, unlike long range order, does not break the ergodicity of the system, $\overline{J}$ is equal to $\overline{J}_{\text{dis}}$ at all temperatures greater than T_{O} in the mean field theory, so that as long as $T_{\text{O}} < T_{\text{C}}$ the value of T_{O} will have no effect on T_{C}. This is illustrated in figure 5.

Because of this dependence of $T_{\text{C}}^{\text{SIM}}$ on V a further adjustment to $J_{\text{tot}}^{\text{NiNi}}$ was made, while retaining the ratios in (8), leading to our final estimates of the interaction values:

$$\begin{aligned} J_{\text{tot}}^{\text{NiNi}} &= 5.3 \text{ meV} \\ J_{\text{tot}}^{\text{NiFe}} &= 11.4 \text{ meV} \\ J_{\text{tot}}^{\text{FeFe}} &= -3.3 \text{ meV} \\ V &= -130 \text{ meV}. \end{aligned} \tag{11}$$

The phase diagram produced by the simulation using these values in conjunction with the relations (2) is shown in figure 4.

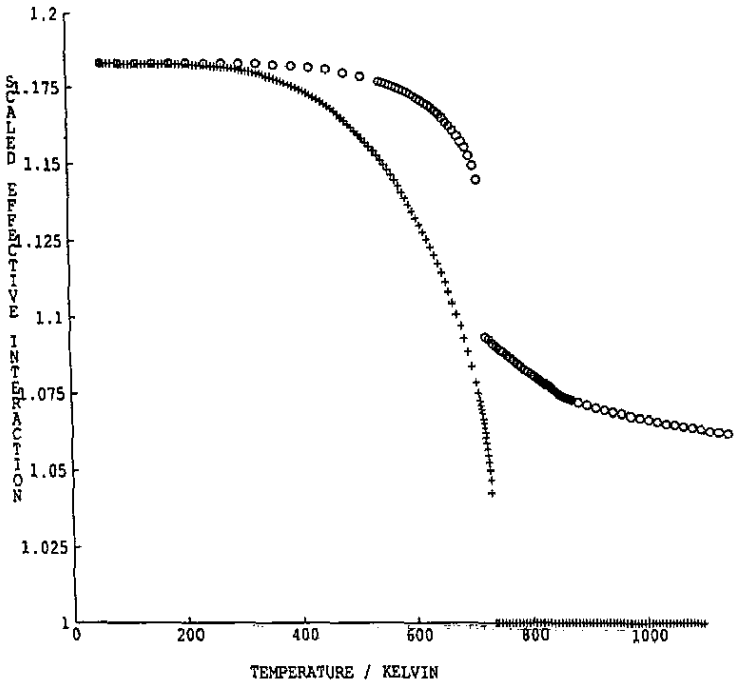

Figure 5. $\overline{J}/\overline{J}_{dis}$ against temperature for simulation and mean field theory. At T_O $\overline{J}$ drops to its disordered value for the mean field theory, but short range order persists above T_O in the simulation. Composition is about 80% Ni. O, simulation; +, mean field approximation.

Fitting the mean field theory to the data of Wakelin and Yates [13] gave exchange interactions J_{tot}^{NiNi}, J_{tot}^{NiFe}, and J_{tot}^{FeFe} which were different by factors of 0.8, 1.2, and 1.6 respectively from the values quoted above, which are based on the data of Crangle and Hallam [10]. This difference is clearly significant, but it is not disastrous; the interactions retain their signs and orders of magnitude, and in particular the Fe–Fe interaction remains antiferromagnetic. These discrepancies may be regarded as a measure of the reliability of our estimates.

There have been several previous estimates of the value of V. The value above agrees well with one derived by Sakurai *et al* [17] from measurement of the elastic constant $C_{11} - C_{12}$ and Bragg–Williams theory of $V = -128$ meV, although a second estimate in the same study based on the elastic constant C_{44} gives $V = -60$ meV. The value obtained from neutron scattering experiments by Lefebvre *et al* [18] is quite different and is discussed in the following subsection.

4.2. Magnetic short range order

In order to assess the actual antiferromagnetism of the FCC iron we examined the values $P(\uparrow\downarrow)_{nn}^{NiNi}$, $P(\uparrow\downarrow)_{nn}^{NiFe}$ and $P(\uparrow\downarrow)_{nn}^{FeFe}$, where $P(\uparrow\downarrow)_{nn}^{XY}$ is the probability that an adjacent pair of sites will have antiparallel spins, given that one is of type X and the other is of type Y. Formally:

$$P(\uparrow\downarrow)_{nn}^{XY} = \frac{1}{12N} \sum_{\langle i,j \rangle} \frac{P(\sigma_i\sigma_j = -1,\ \xi_i = X,\ \xi_j = Y)}{P(\xi_i = X,\ \xi_j = Y)}$$

where the summation is over nearest neighbour pairs. Note that this quantity can equally well be expressed in terms of correlation functions.

Below T_C, in view of the bulk ferromagnetism of the system, we did not expect to find predominantly antiferromagnetic Fe–Fe pairs (i.e. we did not expect $P(\uparrow\downarrow)_{nn}^{FeFe} > 0.5$), but given the relative values of the exchange interactions (11) it seemed reasonable to expect at all temperatures to find $P(\uparrow\downarrow)_{nn}^{FeFe} > P(\uparrow\downarrow)_{nn}^{NiNi} > P(\uparrow\downarrow)_{nn}^{NiFe}$. This was in general the case, but in both mean field theory and simulations, in certain temperature ranges below T_C at high concentrations (above about 78% Ni), surprisingly, we found $P(\uparrow\downarrow)_{nn}^{NiNi} > P(\uparrow\downarrow)_{nn}^{FeFe}$. An explanation of this fact may be that where there are two Fe atoms on adjacent sites, the natural ordering of the system will tend to occupy nearby sites with Ni atoms. In particular, at fairly high bulk Ni concentrations, the four sites adjacent to both Fe atoms will be almost certainly occupied by Ni atoms (we have verified this by mean field calculations). Because of the strongly ferromagnetic nature of the Ni–Fe interaction and the bulk ferromagnetism of the system, below T_C the spins of the two Fe atoms will be ferromagnetically coupled to each other *through* the four sites adjacent to both. Thus nearest neighbour Fe–Fe pairs will behave more ferromagnetically than the value of J_{nn}^{FeFe} would suggest. We were not able to quantify this reasoning in such a way as to demonstrate unambiguously that it is the cause of the anomaly, but it predicts a decrease in $P(\uparrow\downarrow)_{nn}^{FeFe}$ for roughly the temperature and concentration ranges in which the *prima facie* surprising result $P(\uparrow\downarrow)_{nn}^{NiNi} > P(\uparrow\downarrow)_{nn}^{FeFe}$ is observed. Evidently this is an interesting effect, as it apparently cannot be understood without invoking at least three-body correlations.

At temperatures higher than T_C (at least for those sufficiently far above it that the magnetic correlation length is small) the above reasoning fails, and above T_C we see as expected $P(\uparrow\downarrow)_{nn}^{FeFe} > 0.5 > P(\uparrow\downarrow)_{nn}^{NiNi} > P(\uparrow\downarrow)_{nn}^{NiFe}$; the ordering of Fe–Fe pairs is predominantly antiferromagnetic while that of Ni–Ni and Ni–Fe pairs is predominantly ferromagnetic.

4.3. Compositional short range order

For both simulation and mean field theory correlation functions were calculated and recorded for nearest and next nearest neighbour pairs. This is useful both to gain further information concerning the order of the system and for comparison with data from past and possibly future neutron scattering experiments.

We compared our results with some of the experimental findings of Lefebvre *et al* [18], who obtained values of compositional correlation functions by diffuse neutron scattering from a single disordered crystal of $Ni_{0.765}Fe_{0.235}$ at five temperatures between 658 K and 958 K. From this work they were able to provide estimates of the Warren–Cowley short range order parameters $\alpha(r)$ and also, via the approximation due to Clapp and Moss [19, 20], of the chemical interaction $V(r)$.

The agreement between our results and those of Lefebvre *et al* for the values of α for nearest and next nearest neighbours above T_O was quite close (see figure 6). Our model system seems to be slightly more ordered for nearest neighbours and slightly less ordered for next nearest neighbours than the experimental system. A possible explanation runs as follows: due to the long ordering times and fairly short times allowed experimentally for equilibration the experimental system is overall in a more disordered state than equilibrium, whereas care was taken to ensure that data gathered from the simulation were from equilibrium states, explaining the observation that the nearest neighbour short range order is weaker for experiment than for simulation. This reasoning leads to the conclusion that next nearest neighbours ought also to be less

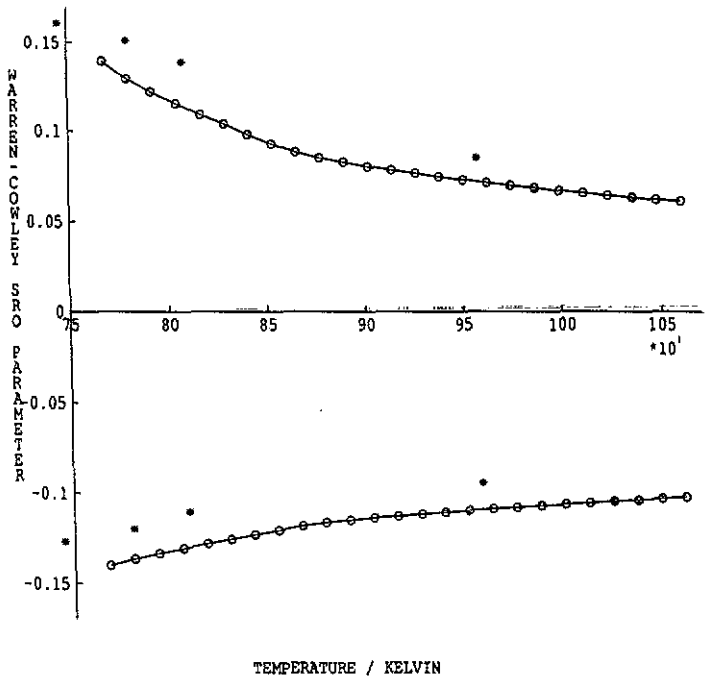

Figure 6. Warren–Cowley order parameters from the simulation and from the neutron scattering data of [18], both around $c = 0.765$. The lower (negative) curve is for nearest neighbours and the upper (positive) one is for next nearest neighbours. O, simulation; *, experiment.

ordered in experiment than in simulation, but the results of Lefebvre *et al* suggest that next nearest neighbour interactions are comparable with nearest neighbour ones rather than negligible as we had supposed, and this could lead to experimental short range order stronger than simulation short range order for next nearest neighbours, as observed.

The value of V_{nn} which they obtained was weakly dependent on temperature and varied also between the two approximations they used to extract it from the experimental data; it is in the region of -50 meV. As a check they calculated the mean field theory values of T_O to which their interactions led, giving values of T_O from 500 K to 940 K (the experimental value is about 770 K).

As noted in subsection 4.1, to fit the experimental ordering temperature our model required $V_{nn} = -130$ meV, a factor of about 2.5 larger than the value of Lefebvre *et al*. The main reason for this discrepancy is the lack of chemical interactions beyond nearest neighbour in our model. We have not calculated the effect of this in detail, but short simulations indicate that if these were included our V_{nn} would be reduced by about a factor of 2.

It may also be the case that the interaction values of [18] are a little low due to the probable non-equilibrium state of the alloy as suggested above. This is suggested also by the T_O values calculated in [18] and mentioned above which one would expect to be higher than the experimental value, since mean field theories always overestimate ordering temperatures, particularly in frustrated systems such as ordering alloys on a FCC lattice. Since the T_O values they calculate are not higher than the experimental

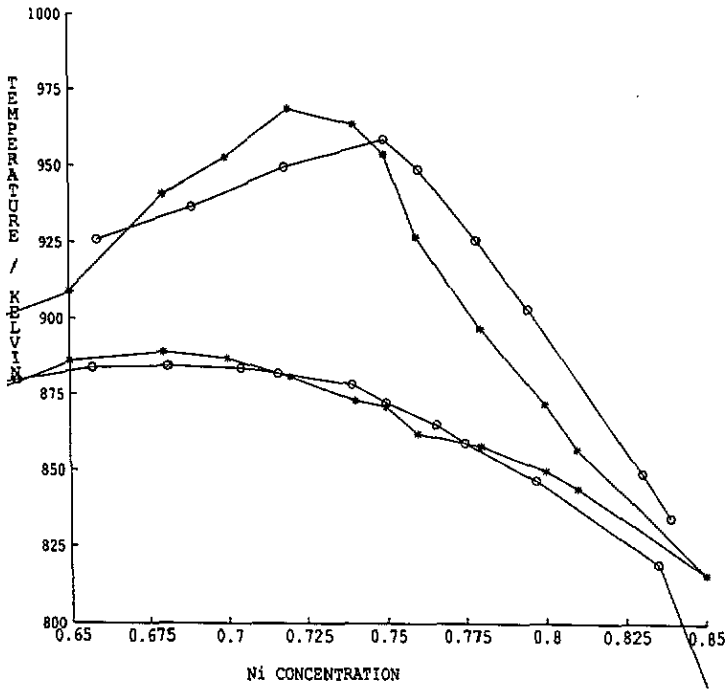

Figure 7. Curie temperatures of the ordered phase (upper curves) and disordered phase (lower curves). O, simulation (using a system with compositional order frozen in); *, experiment (extrapolated from low temperature $M(T)$ curves [13]).

value, it seems likely that their interactions are too weak.

4.4. The temperature dependence of the magnetization

For both the simulation and the mean field theory the dependence of spontaneous magnetization on temperature was examined. In both cases there is an anomaly in the temperature dependence of the magnetization $M(T)$ at T_O. This is presumably because $L1_2$ ordering inhibits antiferromagnetic Fe atoms from occupying adjacent sites, and this order is destroyed above T_O, causing a reduction in the effective exchange interaction (9). Such an anomaly was observed experimentally by Wakelin and Yates [13], and although the form of the anomaly appears to differ somewhat between mean field theory, simulation and experiment the method of quantifying the effect used by Wakelin and Yates permits a comparison of the results. By extrapolating the low temperature (i.e. ordered) portion of $M(T)$ to $M = 0$, they were able to find a set of values $T_C^{ord}(c)$, the Curie temperatures that it appeared the samples would have had if they had remained ordered at high temperatures. They claimed to be able to perform these extrapolations to give T_C^{ord} to an accuracy of ± 5 K. The shape of our simulation curves suggested no appropriate extrapolation to similar levels of accuracy, and so a different method was adopted: the system was annealed (the simulation was run until equilibrium was reached) at a temperature below T_O, then quenched (the compositional configuration $\{\xi_i\}$ was frozen in) and simulations run at higher temperatures allowing only magnetic variations in order to determine the Curie temperature T_C^{ord} of this configuration. A comparison of the simulation and experimental results

for $T_C^{ord}(c)$ and $T_C(c)$ can be seen in figure 7. Agreement is quite good except for the fact that the simulation curve peaks at stoichiometry (75% Ni) while the experimental curve peaks at a somewhat lower concentration.

The anomaly in $M(T)$ at T_O is not seen in the observations of Crangle and Hallam [10], since their samples were quenched from temperatures above T_O and thus were compositionally disordered over the whole temperature range. Of interest in their results however is the finding that with increasing Fe composition $M(T)$ becomes flatter, and so the law of corresponding states is not obeyed. Simulations were performed on a lattice which was quenched as described above but in a compositionally disordered state in order to determine whether this behaviour was a property of the simple model under consideration here. There did appear to be some flattening in the simulation, but it was very slight, and did not follow the same trend with concentration as the results of [10], and it seems likely that the experimental effect has a cause outside the scope of this model, for instance decrease of saturation moment with increase of temperature (see [21], pp 24–5).

5. Conclusion

The model used in this investigation is a simple one; obvious aspects of the system which have been neglected are any variation of the atomic magnetic moments, the vector nature of the magnetic spins, possible variation of the exchange integrals with concentration [22], and many-body interactions. Nevertheless it is able qualitatively to reproduce much of the experimentally observed behaviour of these Ni–Fe alloys, and so it seems likely that it captures some of the essentials of the physical system. Central to many aspects of the system seems to be the antiferromagnetism of the Fe–Fe interaction. Our system does not model the behaviour of real Ni–Fe alloys with sufficient accuracy to enable us to provide accurate values for these interactions, but the exchange interaction between FCC nearest neighbour Fe–Fe pairs seems to be in the region of −4 meV. Although the magnetic interactions alone drive a compositional ordering of the type observed experimentally, in order for the transition to occur at a temperature close to the experimental ordering temperature (when compared with the Curie temperature), the chemical interaction must be an order of magnitude greater than the magnetic interactions.

Acknowledgments

We would like to acknowledge repeated useful conversations with Dr M P Allen. MBT was financially supported by an SERC studentship and the calculations were carried out on the departmental DAP provided by the Computational Science Initiative.

References

[1] Abrahams S C, Guttman L and Kasper J S 1962 *Phys. Rev.* **127** 2052
[2] Weiss P and Foëx G 1911 *J. Physique Radium* **1** 274
[3] Knappwost A and Bockstiegel G E 1953 *Z. Elektrochem.* **57** 700
[4] Gonser U, Meechan C J, Muir A H and Wiedersich H 1963 *J. Appl. Phys.* **34** 2373
[5] Johanson G J, McGirr M B and Wheeler D A 1970 *Phys. Rev.* B **1** 3208

[6] Asano S and Yamashita J 1971 *J. Phys. Soc. Japan* **31** 102
[7] Johnson D D, Pinski F J and Staunton J B 1987 *J. Appl. Phys.* **61** 3715
[8] MacKenzie N D and Young A P 1981 *J. Phys. C: Solid State Phys.* **14** 3927
[9] Cadeville M C and Morán-López J L 1987 *Phys. Rep.* **153** 331
[10] Crangle J and Hallam G C 1963 *Proc. R. Soc.* A **272** 119
[11] Massalski T B (ed) 1986 *Binary Alloy Phase Diagrams* (Metals Park, OH: American Society for Metals)
[12 Domb C and Green M S 1974 *Phase Transitions and Critical Phenomena* vol 3 (London: Academic)
[13] Wakelin R J and Yates E L 1953 *Proc. Phys. Soc.* B **66** 221
[14] Van Deen J K and Van der Woude F 1981 *Acta Metall.* **29** 1255
[15] De Fontaine D and Kikuchi R 1978 *Applications of Phase Diagrams in Metallurgy and Ceramics* NBS special publication 496, (Washington, DC: US Government Printing Office)
[16] Shockley W 1936 *J. Chem. Phys.* **6** 130
[17] Sakurai J, Fujii M, Nakamura Y and Takaki H 1964 *J. Phys. Soc. Japan* **19** 308
[18] Lefebvre S, Bley F, Fayard M and Roth M 1981 *Acta Metall.* **29** 749
[19] Clapp P and Moss S 1966 *Phys. Rev.* **142** 418
[20] Clapp P and Moss S 1968 *Phys. Rev.* **171** 764
[21] *Physics and Applications of Invar Alloys* 1978 (Tokyo: Maruzen)
[22] Staunton J B, Johnson D D and Gyorffy B B 1987 *J. Appl. Phys.* **61** 3693